Recent Advances in Star Formation: Observations and Theory
ASI Conference Series, 2012, Vol. 4, pp 55 – 62
Edited by Annapurni Subramaniam & Sumedh Anathpindika

High mass star formation in the Herschel era: highlights of the HOBYS key program

C. Fallscheer[1,2*]
[1]*University of Victoria, Department of Physics and Astronomy, PO Box 3055, STN CSC, Victoria, BC, V8W 3P6, Canada*
[2]*National Research Council of Canada, Herzberg Institute of Astrophysics, 5071 West Saanich Road, Victoria, BC V9E 2E7, Canada*

Abstract. The formation of massive stars still has many unsolved questions. Here I review some of the many fantastic results that have come about through Herschel observations as part of the Herschel OB Young Stellar Objects Survey (HOBYS). Through this guaranteed time key program, the initial conditions of the high-mass star formation process are studied, providing insight into the earliest stages of how massive stars form and evolve. The specific focus here is on the Rosette Molecular Cloud (RMC) in which the pre- and protostellar objects have been identified and classified. Among the studies presented here are the detection of what may be the identification of massive prestellar cores, a temperature gradient observed across the cloud, and the clump mass function for pre- and protostellar clumps.

Keywords : star formation: high mass – Herschel – HOBYS

1. Introduction

When it comes to star formation, the process for low-mass stars (those stars with main sequence masses less than 8 $M_\odot$) is understood much better than for high-mass stars. In the low-mass case, the process can coarsely be described to begin in starless cores within a molecular cloud which collapses gravitationally to form a prestellar core. This object then turns into a Class 0 protostar characterized in its spectral energy distribution (SED) by a significant contribution from the envelope and circumstellar accretion disk. The Class 0 protostar then transitions through the Class I, II, and III

*email: `Cassandra.Fallscheer@nrc-cnrc.gc.ca`

stages characterized in the SED by the central star becoming more and more dominant compared to the envelope and circumstellar disk.

The process for high-mass stars is far less established, especially at the earliest phases of the formation process. Specifically, the existence of high-mass prestellar cores is an open question. This is one of the motivating questions behind the Herschel imaging survey of OB Young Stellar Objects (HOBYS) guaranteed time key program (PI: F. Motte). By observing all of the regions of massive star formation within 3 kpc of the sun, the data from HOBYS provide a large sample with which the precursors of O and B stars can be identified and studied.

2. Observations - Herschel Space Observatory

The HOBYS guaranteed time key program (Motte et al. 2010) consists of over 100 hours of observations with the Herschel Space Observatory (Pilbratt et al. 2010). Herschel was launched on 14 May 2009 and orbits the Sun in the Earth-Sun L2 point. The

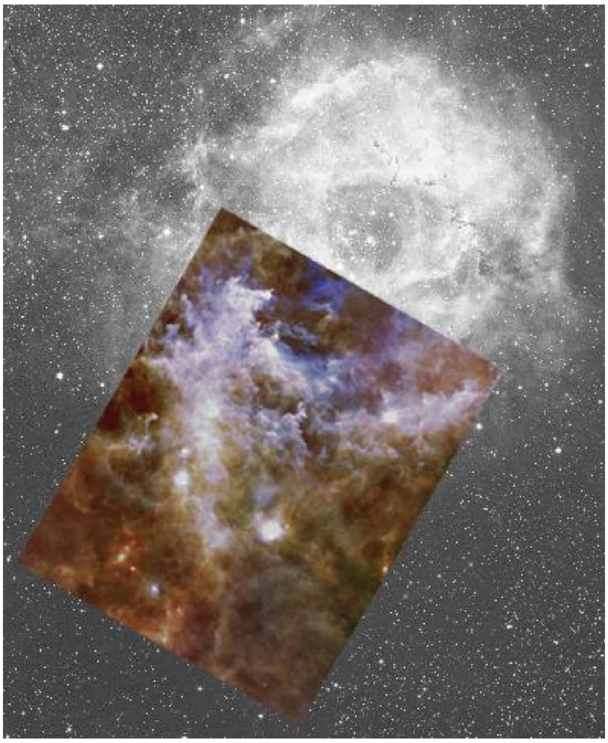

Figure 1. Three color Herschel image (70, 160, 500 μm) overlaid on an Hα image from the Digital Sky Survey. (Credit: Schneider et al., A&A, 518, L83, 2010, reproduced with permission © ESO.)

mirror is 3.5 meters in diameter and there are three scientific data-taking instruments onboard. The two instruments used in the HOBYS project are PACS (Poglitsch et al. 2010) and SPIRE (Griffin et al. 2010). Observations for the HOBYS project were made in parallel mode such that data at 70/160 (PACS), and 250/350/500 (SPIRE) micron were all taken simultaneously. As this wavelength regime includes the spectral energy distribution (SED) peak of young stellar objects, these data are critical in constraining properties of the pre- and proto-stellar objects in the HOBYS survey such as mass, temperature, density, luminosity, etc.

3. HOBYS highlights

3.1 Rosette Molecular Cloud

The Rosette Molecular Cloud (RMC) at a distance of 1.6 kpc is the host of NGC 2244, an HII region within which seven O-type stars are found. Fig. 1 shows the Herschel 3-color image of the RMC region. In this image, red corresponds to the coolest 500 micron emission, 160 micron emission is color coded green, and the warmest gas traced by the 70 micron emission is blue. NGC 2244 is the bright region above the northern edge of the Herschel map. The RMC is often taken as an example of triggered star formation, where gas caught between an expanding HII region's ionization front and shock front fragments into cores from which stars form.

3.1.1 *Protostars in Rosette*

One of Herschel's strengths is classifying and characterizing protostars. Efforts have been made to link the evolutionary stage of prestellar objects in Rosette with their position within the cloud. While a tentative age gradient was reported by Schneider et al. (2010) with the most evolved objects closest to the HII region, other studies (e.g. (Di Francesco et al. 2010)) did not see evidence for such a spread in ages. Fig. 2 plots the envelope mass and luminosity of 88 sources detected by Herschel. This diagram can roughly be used to determine evolutionary stages for the objects in the study. The objects that have a significant envelope mass compared to their luminosity are considered to be Class 0 objects. The central star becomes more dominant as a source evolves, so Class I objects fall below the Class 0 objects in this diagram. Several sources were also identified by Spitzer and were classified by evolutionary type. These classifications are marked as roman numerals over the corresponding Herschel point in Fig. 2. It is interesting to note that approximately half of the Spitzer Class I objects are identified as Class 0 objects based on the Herschel data. This comes about as a result of Herschel better constraining the SEDs of these objects at longer wavelengths where the envelope component contributes significantly. This result is a clear demonstration of one of Herschel's key strengths.

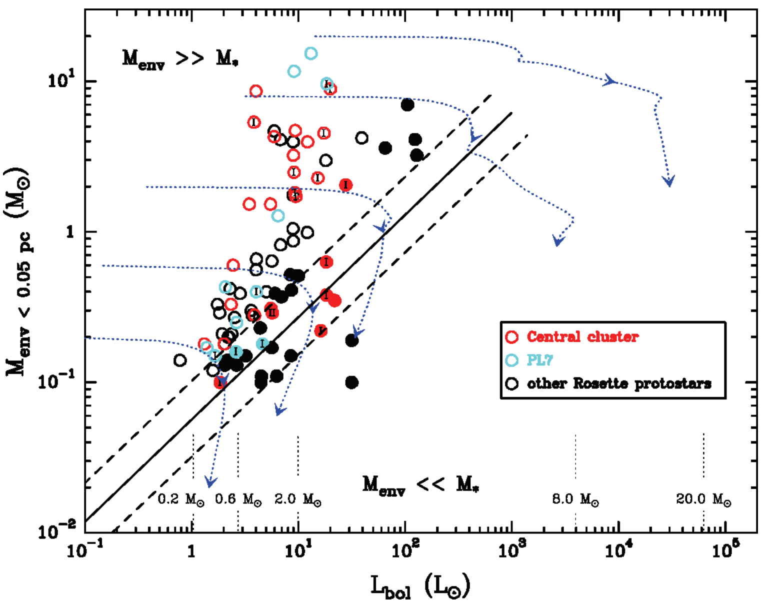

Figure 2. Envelope mass versus bolometric luminosity for a sample of protostars in Rosette. The dotted lines show evolutionary tracks for stellar masses between 0.2 and 20 $M_{\odot}$ and the solid line represents the point where 50% of the mass has been accreted. Open circles denote Class 0 objects and filled circles denote Class I objects. Roman numerals within some of the data points indicate earlier classifications from Spitzer data. (Credit: Hennemann et al., A&A, 518, L84, 2010, reproduced with permission © ESO.)

3.1.2 *Massive Prestellar Cores?*

Another plot of the pre- and protostellar objects in the RMC region is shown in Fig. 3. In this figure, the mass and size of each object is plotted. Motte et al. (2010) determined temperatures and masses for each source by fitting the SED with a grey-body. Those objects of mass higher than 19 $M_{\odot}$ are considered to be possible precursors to massive stars, as they are most likely to produce main sequence stellar masses larger than 8 $M_{\odot}$. Among the nine dense core objects found to be more massive than 19 $M_{\odot}$, three are considered to be prestellar. These three objects are slightly larger and more massive than the objects identified as protostellar. Their high density and slightly cooler temperatures both support the interpretation that these may be prestellar cores. These three are of high interest because if their classification is confirmed, they would represent high-mass analogs to low-mass prestellar cores and hence provide strong clues to the nature of massive star formation.

Follow-up observations to look at these potential prestellar massive cores are currently underway. A program designed for the IRAM 30 meter single dish and Plateau de Bure Interferometer (PI: M. Hennemann) aims to look at these regions at very high

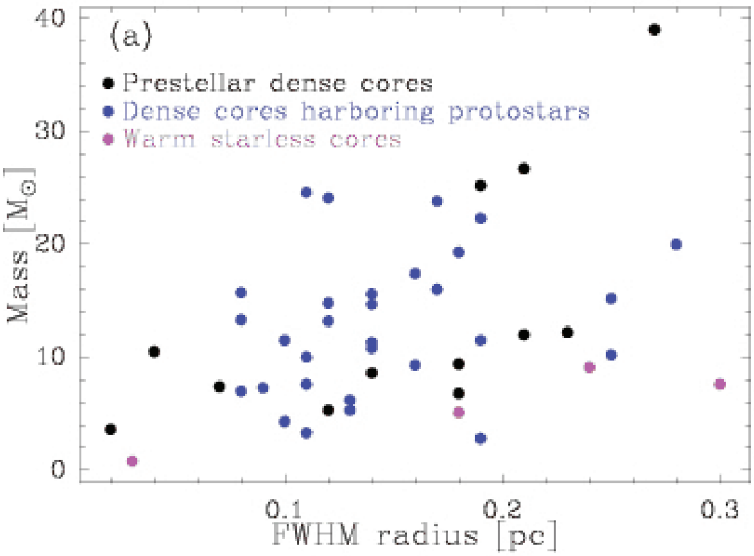

Figure 3. Mass-radius relation for the 46 most massive dense cores in Rosette. (Credit: Motte et al., A&A, 518, L77, 2010, reproduced with permission © ESO.)

angular resolution. It also will detect the local kinematics specifically to see whether these regions are undergoing collapse. Additional observations to determine the temperature structure of of these cores have recently been completed or are currently underway with the Effelsberg telescope (PI: N. Schneider) and the Australia Telescope National Facility (PI: T. Csengeri). These sets of observations will be important for more precisely discovering the properties of these potential high mass cores.

3.1.3 *Temperature Gradient and Mass Function*

Fig. 4 presents the temperature map of the RMC. This figure was produced by fitting a grey-body at each pixel position to the five PACS and SPIRE wavelengths. Schneider et al. (2010) determine through this fitting that the temperature in the region varies between approximately 10 K and 30 K. There is a clear temperature gradient visible in the map with the warmest region (~30K) in the northwest closest to the Hii region and the colder temperatures of 10-15 K furthest away near the cloud's edge.

With its high sensitivity and good spatial resolution at submillimeter wavelengths, Herschel is well suited for studying the origin of the initial mass function (IMF). Herschel is able to resolve the small scale structure within the RMC, and using the *getsources* source extraction algorithm (Men′shchikov et al. 2012), 473 clumps (any object found with a size less than 1 pc) were detected. Using *Spitzer* data, those clumps were further classified as protostellar or starless based on the presence of a

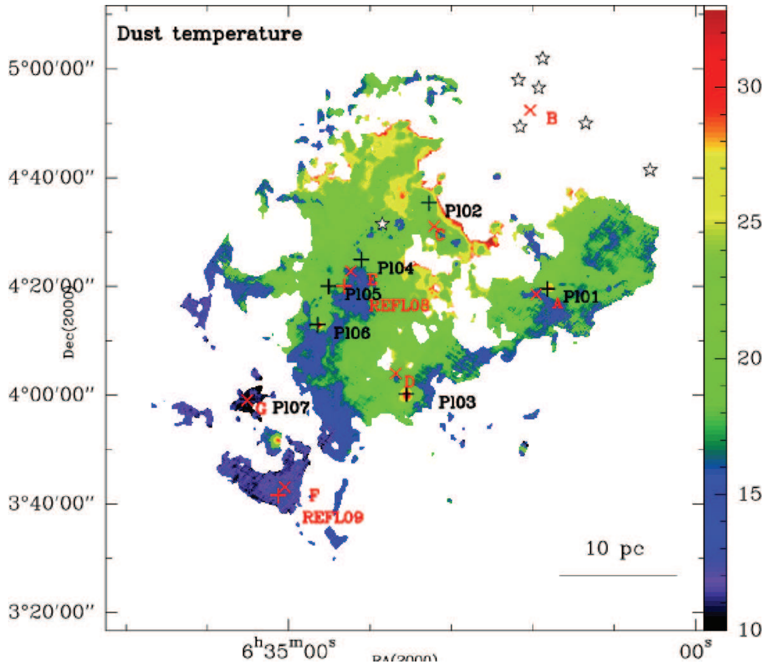

Figure 4. Dust temperature map of Rosette made by fitting all 5 wavebands of the Herschel observations. (Credit: Schneider et al., A&A, 518, L83, 2010, reproduced with permission © ESO.)

young stellar object or not, respectively. Of those clumps detected by *getsources*, 371 were classified as starless and the remaining 102 were considered to be protostellar.

The mass distribution of these clumps is shown in Fig. 5. In this diagram, the starless and protostellar populations are plotted separately. As expected, the starless clumps tend to be less massive than their more evolved protostellar clump counterparts. Of particular interest is the high-mass end of this clump mass spectrum. The slope of the more massive clumps (>1.8 $M_\odot$ for prestellar clumps and >10 $M_\odot$ for protostellar clumps) are computed to be -0.82 for starless clumps and -0.80 for the protostellar clumps. Considering all of the clumps together, the slope is -0.65 - somewhat different from the values for the individual populations because of the different mass regimes those values were calculated from. This is significantly shallower than the Salpeter (1955) value of 1.35, However, these values are comparable to previous slope determinations of the protostellar population of the RMC using CO observations by Schneider et al. (1998) and Dent et al. (2009). Differences to the slopes of mass functions determined for closer regions that agree more closely with the Salpeter value (e.g., Aquila; André et al. 2010) may be a resolution issue. At closer distances, clumps may be resolved further into individual star-forming cores, thereby shifting

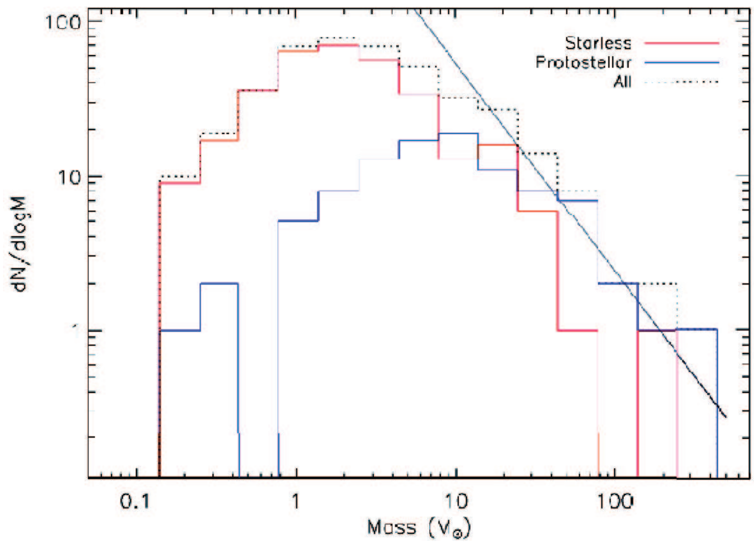

Figure 5. The clump mass function for starless and protostellar clumps in RMC. The Salpeter IMF is shown for comparison as the solid black line. (Credit: Di Francesco et al., A&A, 518, L91, 2010, reproduced with permission © ESO.)

the mass distribution toward lower masses and consequently steepening the high mass end.

3.2 Vela C

The HOBYS key program includes observations of over a dozen regions of high-mass star formation. In these proceedings, however, I will only briefly discuss one other region: Vela C. This molecular cloud complex, located 700 pc away, is the most massive in the Vela region and is currently undergoing both high- and low-mass star formation. Hill et al. (2011, in press) further divide the region up into five sub-regions which they classify as either "ridges" characterized by filamentary structures of high column density, or as "nests". The regions all have roughly the same mass, and should theoretically all be capable of forming high-mass stars. However, it is seen that the most massive stars tend to preferentially form in the higher column density ridges that are likely dominated by self-gravity.

4. Conclusion

With the help of Herschel data, our understanding of the earliest phases of massive star formation is expanding rapidly. Here, I have primarily focused on one of the regions of massive star formation studied in the HOBYS survey. The RMC, host to seven

O-type stars, is a site of ongoing star formation, including high-mass stars. Through identifying sources and fitting SEDs to the multi-wavelength Herschel data, advances have been made in classifying and understanding the objects within high-mass star formation regions. Specifically, Herschel is better able to classify the evolutionary stages of protostellar objects, which is necessary to fully understand the formation process from start to finish. Herschel is able to identify prestellar objects which are likely massive enough to form high-mass stars, although higher resolution imaging will confirm if these are true massive analogues to low-mass prestellar cores. By determining the masses of the clumps within Rosette, a clump mass function was generated exhibiting a slope in the higher-mass regime roughly consistent with previous studies of the RMC, although significantly shallower than the slopes found for closer regions of star formation. Temperature and column density maps are useful indicators of how star formation is progressing in a given region. In the RMC, a temperature gradient with the warmest temperatures found closest to the nearby HII region is discovered, and in Vela C, the column density maps aid in the discovery that the most massive stars tend to form in the filamentary regions of highest column density.

Acknowledgements

I thank the conference hosts for a well-organized meeting and acknowledge funding to attend this conference from a Space Science Enhancement Program grant from the Canadian Space Agency and travel support from the Indian Institute of Astrophysics.

References

André P., et al., 2010, A&A, 518, L102
Dent W. R. F., et al., 2009, MNRAS, 395, 1805
Di Francesco J., et al., 2010, A&A, 518, L91
Griffin M. J., et al., 2010, A&A, 518, L3
Hennemann M., et al., 2010, A&A, 518, L84
Men′shchikov A., et al., 2012, A&A, 542, 81
Motte F., et al., 2010, A&A, 518, L77
Pilbratt G. L., et al., 2010, A&A, 518, L1
Poglitsch A., et al., 2010, A&A, 518, L2
Salpeter E. E., 1955, ApJ, 121, 161
Schneider N., Stutzki J., Winnewisser G., Block D., 1998, A&A, 335, 1049
Schneider N., et al., 2010, A&A, 518, L83